Directing the mechanism of CO_2 reduction by a Mn catalyst through surface immobilization.

James J. Walsh[a,b]*, Mark Forster[c], Charlotte L. Smith[c], Gaia Neri[c], Richard J. Potter[d] and Alexander J. Cowan[c]

Abstract

Immobilization of a Mn polypyridyl CO_2 reduction electrocatalyst on nanocrystalline TiO_2 electrodes yields an active heterogeneous system and also significantly triggers a change in voltammetric and catalytic behaviour, relative to in solution. A combination of spectroelectrochemical techniques are presented here to elucidate the mechanism of the immobilised catalyst in-situ.

Introduction

CO_2 levels in the atmosphere are constantly increasing due to a rapidly expanding world population and industrialization. The use of CO_2 as a commodity for feedstocks and fuels such as CO and CH_3OH is an attractive alternative to carbon capture and sequestration, where the carbon is not reused. CO_2 reduction can be achieved by both photo- and electrocatalytic methods.[1] One of the most well-known molecular CO_2 reduction catalysts is $[Re(bpy)(CO)_3Br]$ and its derivatives, which can be driven either photochemically or electrochemically;[2] however the overpotentials required are often significant (η = 1.0 V), and Re is rare and expensive.

Over the past 6 years analogous Mn complexes have attracted considerable attention as catalysts for homogeneous electrochemical proton-coupled CO_2 reduction at modest overpotentials.[3] Catalysts of the form $[Mn(bpy)(CO)_3X]$ (where X = halide, solvent, pseudohalide; bpy = 2,2'-bipyridyl) favour an electrochemical-chemical-electrochemical (ECE) mechanism, whereby the first one-electron reduction results in X ligand loss accompanied by fast Mn-Mn dimerization yielding $[Mn_2(bpy)_2(CO)_6]$. The second reduction results in dimer cleavage to yield the catalytic five co-ordinate anion $[Mn(bpy)(CO)_3]^-$, see Scheme 1.[4, 5, 6, 7] Catalysis has also been observed to occur in some cases directly via the dimer in a lower-energy pathway.[8] In other cases the mechanism was altered fundamentally by employing bulky 6,6'-disubstituted bpy ligands which sterically prevented dimerization, facilitating the formation of the two-electron reduced species at lower potentials via an EEC mechanism whereby two one-electron transfers occur at the same potential prior to ligand loss.[9, 10]

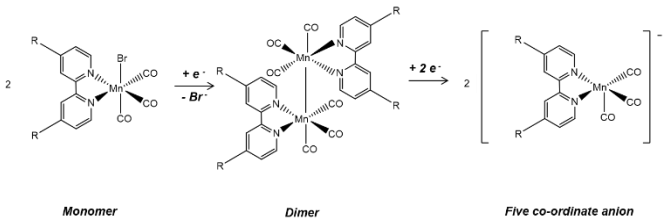

Scheme 1: Generic reduction pathway for $[Mn(bpy(R)_2)(CO)_3Br]$ in solution.

Mn is the 12th most abundant element in the Earth's crust and is thus suitable for scale-up. One key step towards scale-up is to immobilize catalysts on high surface area electrode supports. Immobilization can impart some of the advantages of heterogeneous catalysis such as reusability and fast interfacial electron transfer kinetics. Previously, we have immobilized a variety of complexes of the form $[Mn(bpy(R)_2)(CO)_3Br]$ (where bpy = 2,2'-bipyridyl-4,4'-$(R)_2$; R = H (**1**), ^{t}Bu (**2**), COOH (**3**), OH (**4**)) on glassy carbon electrodes in a Nafion/multi-walled carbon nanotube film for CO_2 reduction in

pH 7 aqueous buffer.[11, 12] Surprisingly we noted in our original studies that despite the complex being deposited on a carbon electrode, following initial reduction dimerization could still take place. Furthermore, it was proposed that CO_2 reduction may have been occurring via both pathways, through both the interaction of $[Mn(bpy)(CO)_3]^-$ with CO_2 and *via* the direct CO_2 insertion into the dimer, $[Mn_2(bpy)_2(CO)_6]$. We subsequently began a study of the direct covalent immobilization of **3** onto mesoporous TiO_2 nanocrystalline (nc) electrode supports to further explore these interesting phenomena. Recently, a report describing the direct covalent immobilization of the closely related complex $[Mn(bpy(PO_3H_2)_2)(CO)_3Br]$ on TiO_2 (hereafter MnP/nc-TiO_2) electrodes was published.[13] Intriguingly, the authors demonstrated a significant change in the voltammetric behaviour of the complex when immobilized, relative to in DMF solution, and catalysis was proposed to only occur via the lower-potential dimer-mediated pathway, although the mechanism of dimer formation on the surface is still not fully understood. Surprisingly no spectroscopic evidence for the formation of $[Mn(bpy(PO_3H_2)_2)(CO)_3Br]^-$ was attained leading the authors to conclude that it was not involved in the mechanism of CO_2 reduction. Herein we expand on this study by presenting a series of spectroelectrochemical (SEC) experiments used to probe the catalyst mechanism *in-situ* using **3**/nc-TiO_2 electrodes. We show that the covalent immobilization of **3** triggers significant changes in the redox chemistry, relative to in solution or when entrapped in a Nafion membrane, and in contrast to related works on MnP/nc-TiO_2, that the five-coordinate anion can be accessed; indeed, it is formed at lower potentials on TiO_2 than typically achieved in solution. We also apply UV/Vis cyclic voltabsorptometry and in-situ ATR-FTIR SEC to directly probe the redox behaviour of **3** on nc-TiO_2, leading to elucidation of the mechanisms occurring when this widely studied class of catalyst is immobilised.

Results and Discussion

Voltammetric properties: TiO_2 nanoparticle films are well known to serve as robust and effective electrodes for adsorbing large quantities of molecular species, most notably in dye-sensitized solar cells,[14] but increasingly for use in solar fuel synthesis as at applied potentials cathodic of the conduction band edge the films become conductive.[15] Films of **3** on nc-TiO_2 were formed by dip-coating electrodes of FTO/nc-TiO_2 (10 µm film thickness) in ca. 10^{-4} M ethanolic solutions of **3**. The geometric surface coverage, Γ, of **3** was calculated using UV/Vis spectroscopy from the decrease in the Mn absorption band of the soaking solution at ca. 420 nm (Fig. S1); Γ values of ~ 1 x 10^{-7} mol/cm^2 were typical. FTIR spectroscopy revealed that the Mn tricarbonyl structure remained intact upon immobilization, and that the complex is bound to the TiO_2 in a bidentate fashion (vide infra).[16]

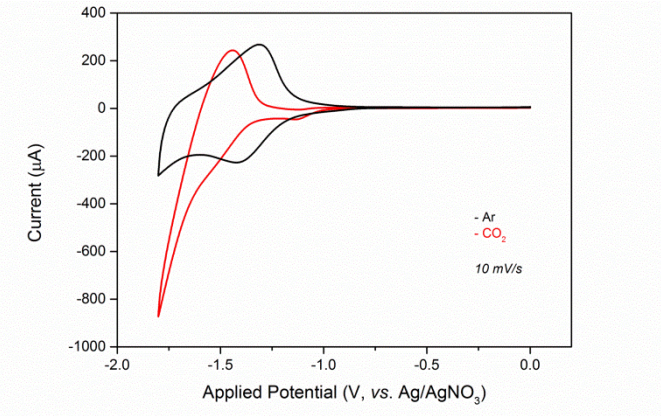

Fig. 1: Cyclic voltammetry in 0.1 M $(But)_4N$ PF_6/CH_3CN supporting electrolyte using a **3**/TiO_2 working, a Pt counter and an $Ag/AgNO_3$ reference electrode. v = 10 mV.s^{-1}.

Cyclic voltammetry (CV) of the films was performed in 0.1 M $(But)_4N$ PF_6/CH_3CN electrolyte and is shown in Fig. 1. It should be noted that the supporting electrolyte and solvent used were not thoroughly dried and therefore a significant proton concentration (< 150 ppm)[17] present can facilitate CO_2 reduction catalysis. Blank nc-TiO_2 films show only capacitive behaviour onsetting at ca. -1.3 V which is assigned to the filling of vacant states close to the conduction band edge (Fig. S2 (b)). The CV of **3**/TiO_2 under Ar in Fig. 1 shows the presence of a large Mn-based reduction peak at -1.45 V and a reoxidation at -1.32 V. Scan rate dependent cyclic voltammetry (Figs. S2, S3) shows a linear dependence on peak current for both features, demonstrating that the complex is adsorbed. In the presence of added CO_2 a catalytic current increase is observed with an onset at ca. -1.6 V. Controlled potential electrolysis at -1.45 V using **3**/TiO_2 resulted in destruction of the underlying FTO glass, as indicated by the formation of a brown colour and a loss in electrical conductivity. This has been seen previously in related studies and attributed to the irreversible reduction of tin.[18] Stabilisation of the underlying FTO was achieved by atomic layer deposition (ALD) of a thin (20 nm) TiO_2 barrier layer onto which a mesoporous TiO_2 film was prepared (see ESI for full details). ALD has been used extensively in recent years as a method to protect the surface of various electrodes and photoelectrodes from corrosion or decomposition,[19] and the **3**/nc-TiO_2/TiO_2(ALD) sample was found to be relatively stable for CO production achieving a turnover number > 6 per Mn centre in the presence of CO_2 at -1.45 V. Experiments under Ar at -1.45 V using identical samples yielded no significant CO confirming that the CO is produced by electrocatalytic CO_2 reduction, at ca. 250 mV positive of that seen in solution previously.[12] We now turn to assigning the mechanism of catalysis. The CV of **3**/nc-TiO_2 is markedly different from that of **3** dissolved in CH_3CN/H_2O (95:5), where two complex reductions are clearly separated by 340 mV (Fig. S4) assigned to the initial reduction of **3** and the subsequent reduction of the dimer complex.[12] It is feasible that the covalent immobilization has (i) prevented dimer reduction in the potential window studied, or (ii) has shifted the two reduction potentials closer together making them closely overlapping. In solution an oxidation at -0.52 V is assigned to dimer oxidation to reform the starting complex (Fig. S4). At potentials greater than ca. -1 V the TiO_2 films are insulating which would rationalise the differences upon immobilisation at these potentials, however as we will show below dimer oxidation can be assigned to the feature at ca. -1.32 V.

UV/Vis spectroelectrochemistry and cyclic voltabsorptometry:

UV/Vis/NIR SEC of **3**/nc-TiO_2 was performed in 0.1 M $(But)_4N$ PF_6/CH_3CN in transmittance mode. Upon polarising the working electrode at -1.4 V a new species was formed with maxima at 640 and 810 nm (Fig. S5), in line-with the previously reported spectrum of the parent dimer $[Mn_2(bpy)_2(CO)_6]$.**3** However assignment is complicated by the presence of the absorption features of electrons trapped in TiO_2 which display a UV/Vis maximum at ~900 nm (Fig. S6).[20] Stepwise measurements 50 mV intervals across the reduction shows a shift in the UV/vis maxima to ca. 460, 610 and 780 nm, with a far greater increase in intensity at 610 nm at more negative potentials. $[Mn(bpy)(CO)_3]^-$ in solution displays absorption maxima at 375, 560 and 626 (sh) nm in MeCN. The combination of the intense band at 610 nm and the shoulder at 780 nm suggest the formation of the five-coordinate anion, with spectral combinations from residual dimer and/or trapped electrons in nc-TiO_2. Clearly, the difference in the shape of the UV/Vis spectra as the potential changes suggests that the stepwise formation of multiple products can occur upon reduction between - 1.3 and - 1.7 V. To further investigate the possibility of the reduction consisting of two distinct redox processes, differential cyclic voltabsorptometry (DCVA) was performed. This involves recording an optical response as the applied potential is modulated. The derivative of the measured absorption provides a quantitative measure of the rate of change of concentration of an electrochemically generated species, making it directly comparable to the current-voltage plot. Because the optical signal recorded is relatively free from background contribution, redox transitions become well defined and capacitance contributions are

eliminated. This technique has been used to great effect particularly in protein film electrochemistry.[21]

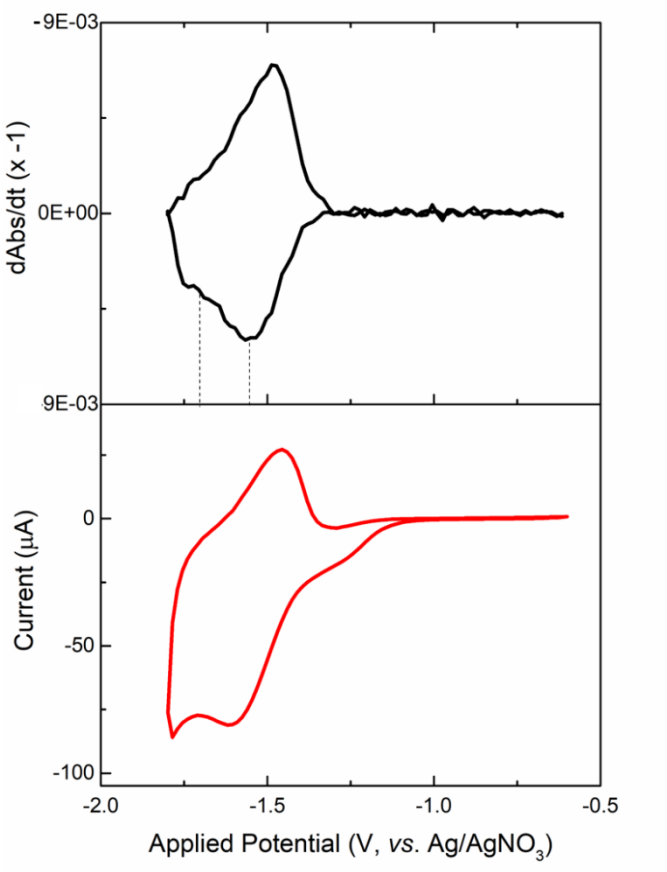

Fig. 2 (a): Derivative absorbance change at 603 nm and (b) corresponding CV at 10 mV.s^{-1} under an argon atmosphere.

The DCVA of **3**/TiO_2 recorded at 603 nm is shown in Fig. 2 (a). The positive derivative absorption upon initial reduction (note the axis is inverted as per convention with DCVA measurements)[21] shows the growth of new species with absorptions at 603 nm. Notably two peaks, separated by ca. 150 mV (ca. -1.55 and -1.70 V), are observed during the initial reduction indicating that two sequential reductions occur which are not readily observed by CV measurements alone (single reduction at ca. -1.61 V, Fig. 2(b)). During the re-oxidation two distinct steps are not clearly present. Steady state SEC indicates that the starting **3**/nc-TiO_2 is reformed. This may either be a two-electron concerted oxidation or two sequential one-electron oxidations that are closely spaced and not well resolved in this experiment. 603 nm was chosen as the probe wavelength as both proposed electrochemically generated species can be monitored at this wavelength, and it does not overlap with the maximum absorbance of trapped electrons in nc-TiO_2 (Fig. S6). Given that ΔAbs returns to zero on the reverse sweep, the reoxidation appears fully reversible (i.e.: after one full cycle no absorbance corresponding to either reduced Mn species or trapped nc-TiO_2 electrons remains).

ATR-FTIR spectroelectrochemistry: DCVA experiments demonstrate the presence of two distinct steps upon the reduction of **3** on nc-TiO_2. It is anticipated that these would be due to initial formation of the dimer species followed by reduction to a five-coordinate anion. Whilst the UV/Vis spectrum of the initial reduction product does correlate well with the known solution spectrum of the dimer the 2nd reduction product remains unassigned. FTIR spectroscopy of the *ν*(CO) modes of **3**/nc-TiO_2 provides a

route to accurate assignment of the reduction mechanism. *In-situ* ATR-FTIR SEC studies on a **3**/nc-TiO_2 film were carried out as shown in Scheme 2 (details in ESI).

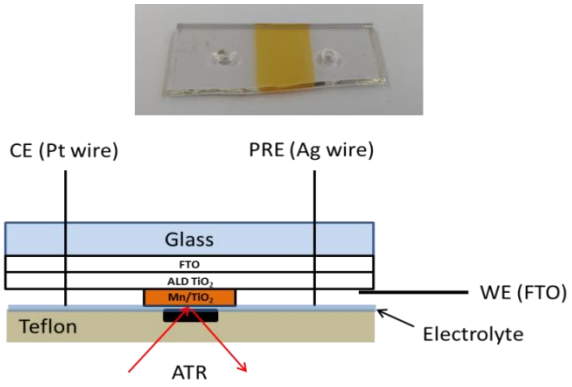

Scheme 2: Photo and schematic diagram of cell setup for *in-situ* ATR FTIR SEC using drilled **3**/TiO_2 film. Layer thicknesses not to scale.

The ATR-FTIR SEC responses are shown in Fig. 3. Assignments of the spectroscopic features are made by direct comparison with the SEC of homogeneous **2** in CH_3CN measured in a thin layer cell reported previously.[22] The spectrum in Fig. 3 (black, at OCP) shows the adsorbed starting monomeric complex (**3**/nc-TiO_2) (2030, 1932 (br) cm^{-1}). Also present is **3**/nc-TiO_2 where the Br^- ligand has been replaced by a solvent ligand (i.e.: $[Mn(bpy(COO)_2)(CO)_3(MeCN)]^+$; *ν*(CO) at 2048 and 1947 (br) cm^{-1}).[12] Initially upon reduction (Fig. 3, red) the formation of a dimeric species is observed with bands at 2025 (w), 1970, 1927, 1875, 1847 and 1808 (w) cm^{-1}, confirming the UV/Vis SEC assignment, and which is in-line with the previous reported MnP/nc-TiO_2 system.[13] We also observe a 2nd reduction product formed subsequently with *ν*(CO) at 1805 and 1905 cm^{-1} which can be readily assigned to the five co-ordinate anion $[Mn(bpy(COO)_2)(CO)_3]^-$ (Fig. 3, blue), with some residual dimer modes still present. A comparison between the assignments and literature values of *ν*(CO) bands of related species is given in Table S1.

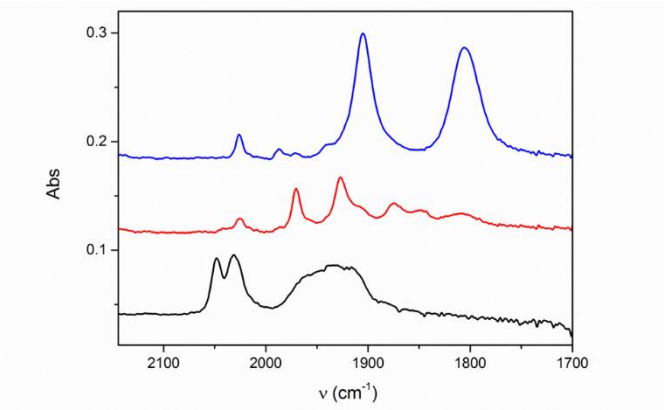

Fig. 3: ATR-FTIR spectroelectrochemistry of **3**/TiO_2 showing the monomer (black) dimer (red) and five co-ordinate complex (blue).

Despite the considerable differences in CV of **3** upon immobilization on TiO_2 this sequence of redox processes mirrors the ECE mechanism usually observed in solution and conclusively demonstrates dimerization of **3** on TiO_2 which can then be subsequently reduced. Confirmation that catalysis can

occur *via* the dimeric pathway has been shown previously by bulk electrolysis of Mn solutions under an Ar atmosphere to produce the dimer, positively identified *in-situ* by UV/Vis.[8] Catalytic consumption of dimeric **3** on TiO_2 was also monitored by this method through loss of dimer absorbance at 647 nm upon CO_2-purging (Fig. S7) and it is apparent that when immobilised this Mn complex is still able to reduce CO_2 by both the previously reported dimeric pathway and through the formation of $[Mn(bpy)(CO)_3]^-$, the commonly observed pathway in solution.

Discussion: The immobilization of **3** on TiO_2 alters the electrochemical response relative to solution. The formation of Mn-Mn dimers on the surface, as observed for both **3**/TiO_2 and MnP/TiO_2,[13] is somewhat surprising giving the restricted geometry of surface bound complexes, nonetheless, we confirm here that **3** dimerises on nc-TiO_2. Dimerization can potentially occur in three ways: (a) proximity dimerization, whereby two chemisorbed monomer complexes are reduced, lose a bromide, and are sufficiently close to form a new Mn-Mn bond; (b) the complexes are only weakly physisorbed, and can therefore freely diffuse into the necessary configuration to dimerise; (c) the monomer is chemisorbed and upon electrochemical reduction loses a bromide, desorbs, reorients, dimerises, and then potentially re-adsorbs.

Mechanism (a) appears unlikely on the grounds of both the near complete conversion of the starting material into its dimeric form as measured by FTIR spectroscopy (Fig. 3) and the typical Mn-Br (2.5 Å)12 and Mn-Mn (2.9 Å) bond lengths, as measured by X-ray crystallography,[23] strongly implying that one or both monomers must physically move to dimerise. Mechanism (b) can be excluded as FTIR spectroscopy of **3**/TiO_2 in the fingerprint region shows that the carboxylic acid groups are bound in a bidentate fashion,[16] while the absence of other binding carbonyl modes suggests that this binding geometry dominates (Fig. S8). This leaves mechanism (c) as the most likely case. Given that the scan rate dependent CV data are linear across multiple CV cycles we can infer that electrochemical cycling, regardless of the mechanism, does not trigger permanent desorption of the complex into solution in appreciable quantities, otherwise the data in Fig. S3 would be non-linear. Combining these datasets, we postulate the following mechanism (Scheme 3): the monomer complex **3** is chemisorbed onto TiO_2 *via* a bidentate carboxylate linkage, as shown by FTIR binding mode analysis. Upon the first one-electron reduction and bromide loss, reduced radical **3** desorbs at least sufficiently to enable re-orientation. The desorbed radical complex dimerises and either re-binds to the TiO_2 surface immediately prior to or post formation based on the scan rate dependence of the reoxidation feature of this complex. This dimerization rate constant for the parent complex **1** in CH_3CN solution has been measured on the order of 109 $M^{-1}.s^{-1}$ previously using time-resolved FTIR spectroscopy,[24] so dimerization likely occurs in close proximity to the surface (i.e.: within the diffusion layer or nc-TiO_2 mesopores). It is clear from the FTIR spectrum of the adsorbed dimer on nc-TiO_2 (Fig. 3, red) that the adsorbed dimer occupies the same point group as dimeric **2** free in solution, implying that the dimer is bound to the nc-TiO_2 through one of the two dimer bpy ligands only, with the other ligand rotated and pointing away from the surface (this is also the least sterically hindered confirmation the dimer can adopt). The subsequent reduction, measured by DCVA as ca. 150 mV negative of the potential of dimer formation, results in the formation of the doubly reduced anion. Assignment of the 2nd reduction to this feature is based primarily off FTIR data with the UV/Vis SEC showing similar but slightly shifted spectral features to similar complexes in solution; [13, 22] however it is important to note that the presence of strong electron withdrawing groups (-COO-) on the bipyridine ligand, coupled to changes in electronic structure occurring following covalent attachment to nc-TiO_2, are likely to significantly shift the energy of the MLCT transition being probed. This species can be fully reoxidised to the adsorbed monomer, as shown by UV/Vis SEC (Fig. S5)

The ability to form the five-coordinate anion may appear to contrast with past studies on the related system MnP/nc-TiO_2 in which only a single reduction product was reported (a MnP dimer); however, we highlight that SEC experiments in that case were carried out under CO_2. Similar to past work[8] we find that the Mn dimer is catalytically active towards CO_2 as demonstrated by the loss in dimer absorption at 647 nm upon CO_2 purging (Fig. S7), and confirmed by GC measurements. However dimer mediated CO_2 reduction is likely not the sole catalytic pathway available as any TiO_2 bound $[Mn(bpy(COO)_2)(CO)_3]^-$ would be expected to rapidly react with CO_2 which would prevent the build-up of this species during SEC experiments under CO_2. Intriguingly, our CV and spectroelectrochemical studies of the re-oxidation of the five-coordinate anion to reform the parent material (Fig. S5) show no strong evidence for separate electron transfers occurring sequentially, as in the reductive sweep. The re-oxidation therefore potentially occurs *via* a concerted two electron transfer or two sequential one electron transfers at the same or very similar potentials. At present this is not fully understood but the suppression of dimer formation has been observed by CV in the presence of a Brønsted acid (water) previously for **1**,[3] **3**,[12] and the closely related $[Mn(bpy(Me)_2)(CO)_3Br]$ (where $(bpy(Me)_2)$ = 4,4'-dimethyl-2,2'-bipyridyl),[3] and our CVs of **3**/nc-TiO_2 were recorded in the presence of protons. It may be that the reduced complexes can react with H^+ during re-oxidation – in recent times both electrocatalytic H_2 evolution[25] and metal hydride formation[26] have been observed with Mn imine complexes. The phenomenon of dimer suppression, which has been observed over a range of bpy-based complexes, will therefore be studied in further detail in future work.

Conclusions: The electrochemical behaviour of the Mn tricarbonyl complex **3** on nc-TiO_2 electrodes has been assessed using a combination of scan rate dependent cyclic voltammetry, UV/Vis differential cyclic voltabsorptometry, *in-situ* UV/Vis/NIR and ATR-FTIR spectroelectrochemistries, and CO_2 reduction electrocatalysis monitored with gas chromatography and spectroelectrochemistry. The combination of these techniques yielded important new insights into the reaction mechanism of **3** immobilized on nc-TiO_2, relative to the behaviour of **3** in solution, and a change from a solution ECE mechanism to a mechanism involving at least a partial desorption is postulated. It is likely that a similar mechanism takes place in the case of MnP/TiO_2 reported recently.[13] The unique combination of these experiments can potentially be extended to other immobilized molecular catalysts for solar fuels reactions *in-situ*. In future, electrochemical transient absorption spectroscopy, on the nanosecond to millisecond timescales, will be applied to further investigate mechanistic details of Mn polypyridyl complexes for use in electrocatalysis and photoelectrocatalysis.

Notes and references

Acknowledgements: JJW and AJC acknowledge the EPSRC (EP/K006851/1) for a funding and a fellowship respectively. GN thanks the University of Liverpool for funding. Thanks to Prof. Dmitry Shchukin (SIRE) for providing access to the FTIR.

1 A. J. Morris, G. J. Meyer and E. Fujita, Acc. Chem. Res., 2009, 42, 1983–1994.

2 B. Kumar, J. M. Smieja and C. P. Kubiak, J. Phys. Chem. C, 2010, 114, 14220–14223.

3 M. Bourrez, F. Molton, S. Chardon-Noblat and A. Deronzier, Angew. Chem. Int. Ed. Engl., 2011, 50, 9903–6.

4 J. Agarwal, C. J. Stanton III, T. W. Shaw, J. E. Vandezande, G. F. Majetich, A. B. Bocarsly and H. F. Schaefer III, Dalt. Trans., 2015, 44, 2122–2131.

5 J. Agarwal, T. W. Shaw, H. F. Schaefer and A. B. Bocarsly, Inorg. Chem., 2015, 54, 5285–5294.

6 J. Agarwal, T. W. Shaw, C. J. Stanton, G. F. Majetich, A. B. Bocarsly and H. F. Schaefer, Angew. Chemie - Int. Ed., 2014, 53, 5152–5155.

7 F. Franco, C. Cometto, F. Ferrero Vallana, F. Sordello, E. Priola, C. Minero, C. Nervi and R. Gobetto, Chem. Commun., 2014, 50, 14670–14673.

8 M. Bourrez, M. Orio, F. Molton, H. Vezin, C. Duboc, A. Deronzier and S. Chardon-Noblat, Angew. Chem. Int. Ed. Engl., 2014, 53, 240–3.

9 M. D. Sampson, A. D. Nguyen, K. a Grice, C. E. Moore, A. L. Rheingold and C. P. Kubiak, J. Am. Chem. Soc., 2014, 136, 5460–71.

10 K. T. Ngo, M. McKinnon, B. Mahanti, R. Narayanan, D. C. Grills, M. Z. Ertem and J. Rochford, J. Am. Chem. Soc., 2017, 139, 2604–2618.

11 J. J. Walsh, G. Neri, C. L. Smith and A. J. Cowan, Chem. Commun., 2014, 50, 12698–12701.

12 J. J. Walsh, C. L. Smith, G. Neri, G. F. S. Whitehead, C. M. Robertson and A. J. Cowan, Faraday Discuss., 2015, 183, 147–160.

13 T. E. Rosser, C. D. Windle and E. Reisner, Angew. Chemie - Int. Ed., 2016, 55, 7388–7392.

14 M. Grätzel, J. Photochem. Photobiol. C Photochem. Rev., 2003, 4, 145–153.

15 M. Schreier, J. Luo, P. Gao, T. Moehl, M. T. Mayer and M. Gr??tzel, J. Am. Chem. Soc., 2016, 138, 1938–1946.

16 C. Bauer, G. Boschloo, E. Mukhtar and A. Hagfeldt, J. Phys. Chem. B, 2002, 106, 12693–12704.

17 D. B. G. Williams and M. Lawton, J. Org. Chem., 2010, 75, 8351–8354.

18 J. D. Benck, B. A. Pinaud, Y. Gorlin and T. F. Jaramillo, PLoS One, , DOI:10.1371/journal.pone.0107942.

19 S. Hu, N. S. Lewis, J. W. Ager, J. Yang, J. R. McKone and N. C. Strandwitz, J. Phys. Chem. C, 2015, 119, 24201–24228.

20 G. Neri, J. J. Walsh, C. Wilson, A. Reynal, J. Y. C. Lim, X. Li, A. J. P. White, N. J. Long, J. R. Durrant and A. J. Cowan, Phys. Chem. Chem. Phys., 2015, 17, 1562–1566.

21 Y. Astuti, E. Topoglidis, G. Gilardi and J. R. Durrant, Bioelectrochemistry, 2004, 63, 55–59.

22 J. M. Smieja, M. D. Sampson, K. A. Grice, E. E. Benson, J. D. Froehlich and C. P. Kubiak, Inorg. Chem., 2013, 52, 2484–2491.

23 D. W. Agnew, M. D. Sampson, C. E. Moore, A. L. Rheingold, C. P. Kubiak and J. S. Figueroa, Inorg. Chem., 2016, 55, 12400–12408.

24 D. C. Grills, J. a Farrington, B. H. Layne, S. V Lymar, B. a Mello, J. M. Preses and J. F. Wishart, J. Am. Chem. Soc., 2014, 136, 5563–5566.

25 M. D. Sampson and C. P. Kubiak, Inorg. Chem., 2015, 54, 6674–6676.

26 B. Reuillard, K. H. Ly, T. E. Rosser, M. F. Kuehnel, I. Zebger and E. Reisner, J. Am. Chem. Soc., 2017, 139, 14425–14435.